Supporting Information for

Dioxins in the Arctic: local sources vs. long-range transport

Gou et al.

S1 PCDD/Fs emission from anthropogenic sources

Following Song et al. [1], we firstly employed a multiple linear regression model to estimate national atmospheric emissions of PCDD/Fs in the world, defined by

$$\log E_{n,y} = \alpha + C_1 \log Area_n + C_2 \log GNI_{n,y} + C_3 \log ppGNI_{n,y} + C_1 \log CO_2pGDP_{n,y} + \varepsilon \quad \text{(S1)}$$

where n, y represents country and year, respectively, $E_{n,y}$ represents the emissions in year y from country n at unit g TEQ, $Area_n$ is the land area of country n, $GNI_{n,y}$ is the gross national income of country n in year y, $ppGNI_{n,y}$ is the per capita gross national income of country n in year y, $CO_2pGDP_{n,y}$ is the CO_2 emissions per unit GDP of country n in year y, α, C_1, C_2 and C_3 represent model coefficients, and ε is a random error. The PCDD/Fs emission at the national level were collected from the Stockholm Convention website (http://chm.pops.int/), public information of national environmental protection ministries, and literatures. Land area, gross national income (GNI), GNI per capita (ppGNI), and CO_2 emissions per unit GDP ($ppCO_2pGDP$) were collected from the World Bank (www.data.worldbank.org) and the United Nations (http://unstats.un.org).

Secondly, we obtained national PCDD/Fs emission from seven key emission sectors from anthropogenic activity, including waste incineration, ferrous and nonferrous metal production, heat and power generation, production of mineral products, transportation, open-burning processes, production of chemicals and consumer goods, and miscellaneous sectors, by estimating the contribution fraction of each sector to total PCDD/Fs emissions for each country from the literature. By using the composition profile of 17 homologs, we extended sectoral PCD/Fs emission inventories to 17 homologs.

Thirdly, we used the gridded surrogate data to allocate national-level 17 PCDD/Fs

congener emission data to a spatial grid map at a 1◦× 1◦ resolution. More detailed method descriptions can be found in Song et al. [1].

S2 PCDD/Fs emission from wildfire biomass burning

Following the method estimating global benzo[a]pyrene (BaP) emissions from wildfire [2], we estimated global atmospheric emissions of PCDD/Fs from wildfire biomass burning using data derived from satellite products and emission factors (EFs) from biomass burning, defined by

$$E_{c,g,m} = \sum_{i=1}^{n} BA_{i,g,m} \times FL_{i,g,m} \times EF_{c,i} \times CE_i \quad (1)$$

where c, g, m, and i represent PCDD/Fs congener, grid location, month, and vegetation type, respectively. $E_{g,m}$ represents PCDD/Fs emissions from wildfire biomass burning in m at g (kg); $BA_{i,g,m}$ is the burned area in m at g for vegetation i (m^2), determined according to the interaction between vegetation areas (from Moderate Resolution Imaging Spectroradiometer (MODIS) product MCD12Q1) and burnt areas (from MODIS product MCD64CMQ) (Fig. S1); $FL_{i,g,m}$ is the aboveground carbon stock (kg m^{-2}) for vegetation type i, derived from the Global Forest Resources Assessment (https://www.fao.org/forest-resources-assessment/en/) and the MODIS satellite dataset MOD17A3H (https://lpdaac.usgs.gov/product_search/); $EF_{c,i}$ is the emission factor for congener c from vegetation type i; and CE_i is the combustion efficiency of vegetation type i. EFs for forest and grassland burning were collected from the literatures and are listed in **Table S1**. More detailed descriptions for calculating emissions of toxic chemicals from wildfire biomass burning based on burned areas derived from satellite products and emission factors can be found in Song et al. [2].

Table S1. Emission factors (ng TEQ kg^{-1}) of PCDD/Fs from forest and grassland biomass burning

Biomass type	Measuring methods	Emission factor	References
Eucalypt woodland	Field observation	0.12	[3]
Hardwood deciduous forest	Field observation	1.3	[4]
Pine forest	Field observation	0.8	[4]
Pine Forest	Laboratory simulation	0.4	[4]
Pine forest	Field observation	0.5	[5]
Hardwood deciduous forest	Field observation	0.95	[5]
Hardwood deciduous forest	Field observation	1.1	[5]
Pine needles, Hemlock needles	Field observation	2	[6]
Forest fires		1	[7]
Grasses	Laboratory simulation	0.11	[8]
grass/ sugar gum understory	Field observation	0.4	[5]
grass/ sugar gum understory	Field observation	0.26	[5]
grass/ sugar gum understory	Laboratory simulation	0.56	[5]
Grassland and savannah		0.5	[7]
Grasses		0.31	[8]

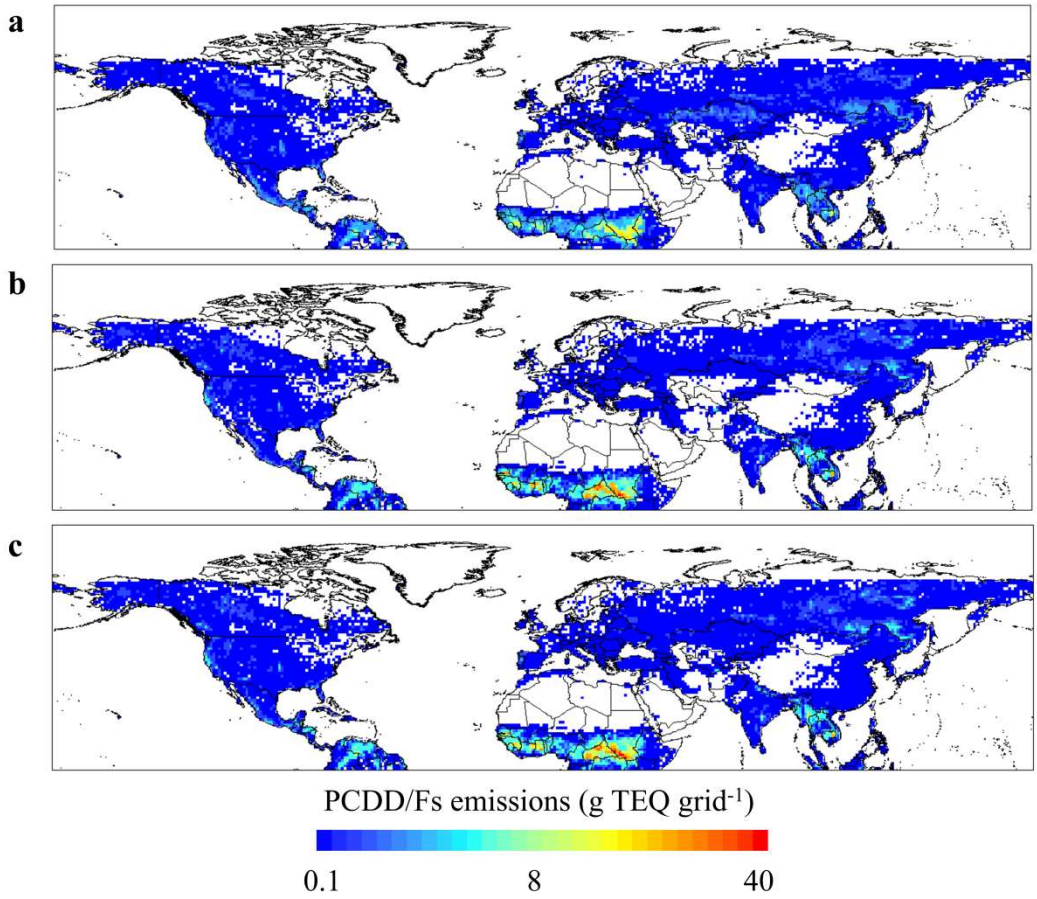

Figure S1. Annual mean PCDD/Fs emissions in the NH averaged over 2011 to 2020 for grassland wildfires only (**a**), forest wildfires only (**b**), and total wildfires (forest + grass fires) (**c**).

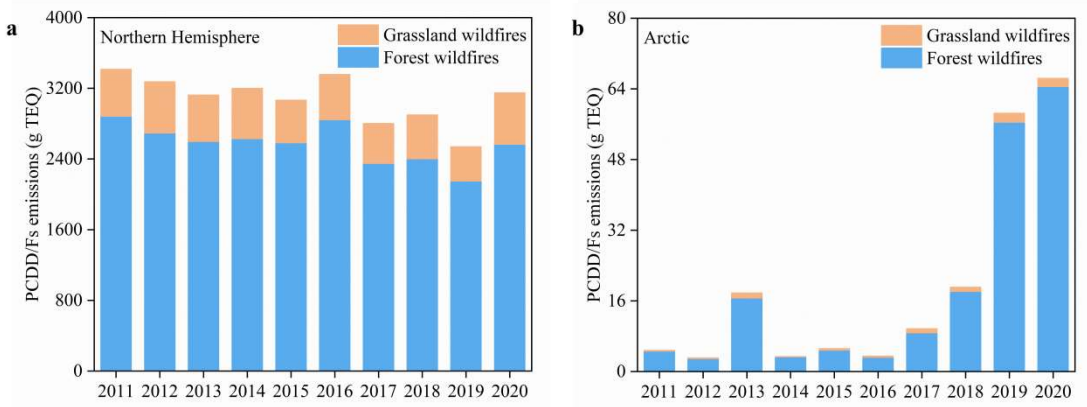

Figure S2. Atmospheric PCDD/Fs emissions from wildfire biomass burning from 2011 to 2020 in the NH (**a**) and the Arctic (**b**).

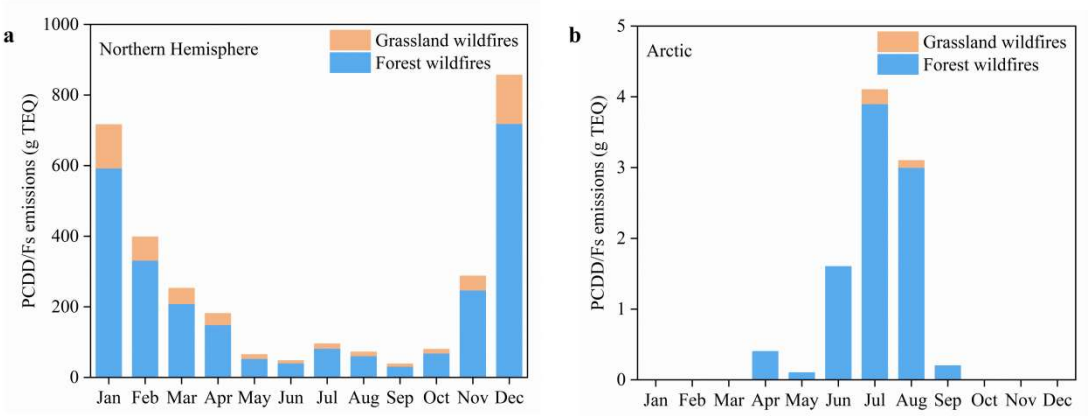

Figure S3. Monthly averaged PCDD/Fs wildfire emissions from 2011 to 2020 in the NH (**a**) and the Arctic (**b**).

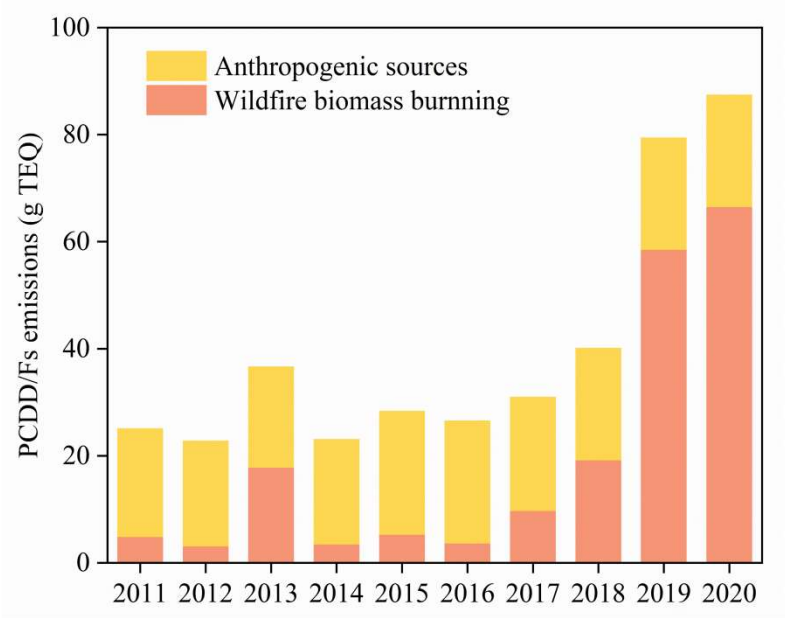

Figure S4. Annual PCDD/Fs emissions from anthropogenic sources and wildfire biomass burning in the Arctic from 2011 to 2020.

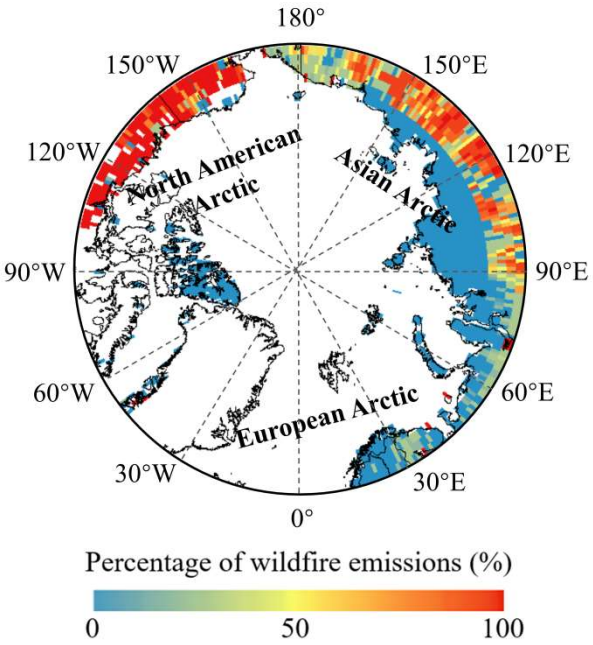

Figure S5. Fractional contributions of wildfire biomass burning to the total PCDD/Fs emission.

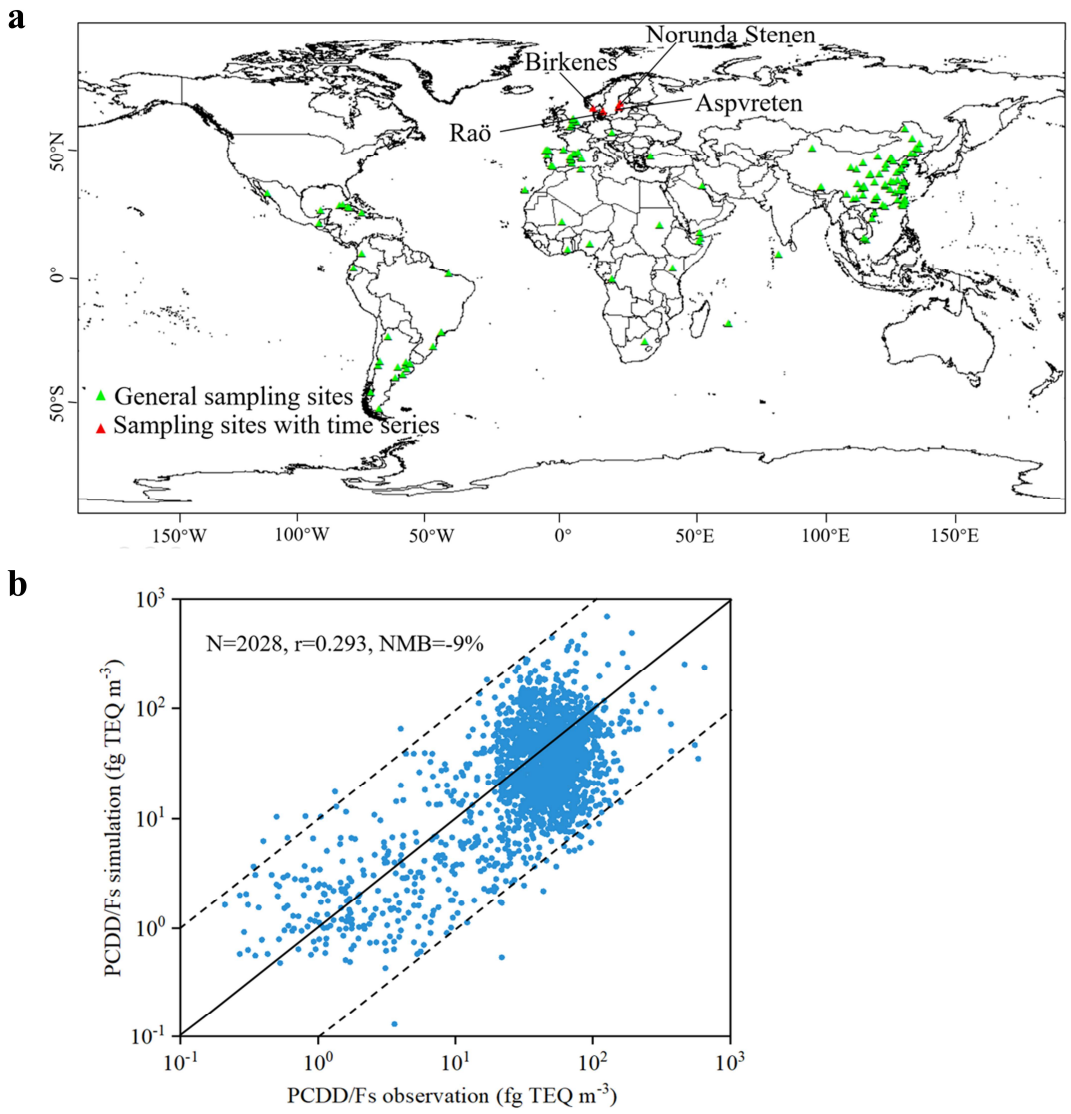

Figure S6. Sampling sites and comparisons between modeled and measured PCDD/Fs air concentrations. **a**. Sampling sites assembled from various field campaigns by different research groups and from literature. The four red triangle denotes the sampling sites where sampled PCDD/Fs concentration with time series were used to compare with the modeled data. **b**. Scatter plot of modeled and measured PCDD/Fs air concentrations. The solid black line represents a 1:1 relationship, and the dashed black lines denote the boundaries where simulated concentrations are 0.1 and 10 times of measured concentrations. The normalized mean bias (NMB) between the modeled and measured PCDD/Fs concentrations was defined as $(\sum_{i=1}^{N}|M_i - O_i|) \times 100/\sum_{i=1}^{N} O_i$, where M_i is ith (i = 1, . . ., N, where N is the number of the simulated data) modelled concentration. O_i is ith (i = 1, …, N, where N is the number of the measured data) measured concentration. All modeled and measured air PCDD/Fs concentrations for comparison are presented in **Supporting Data S1**.

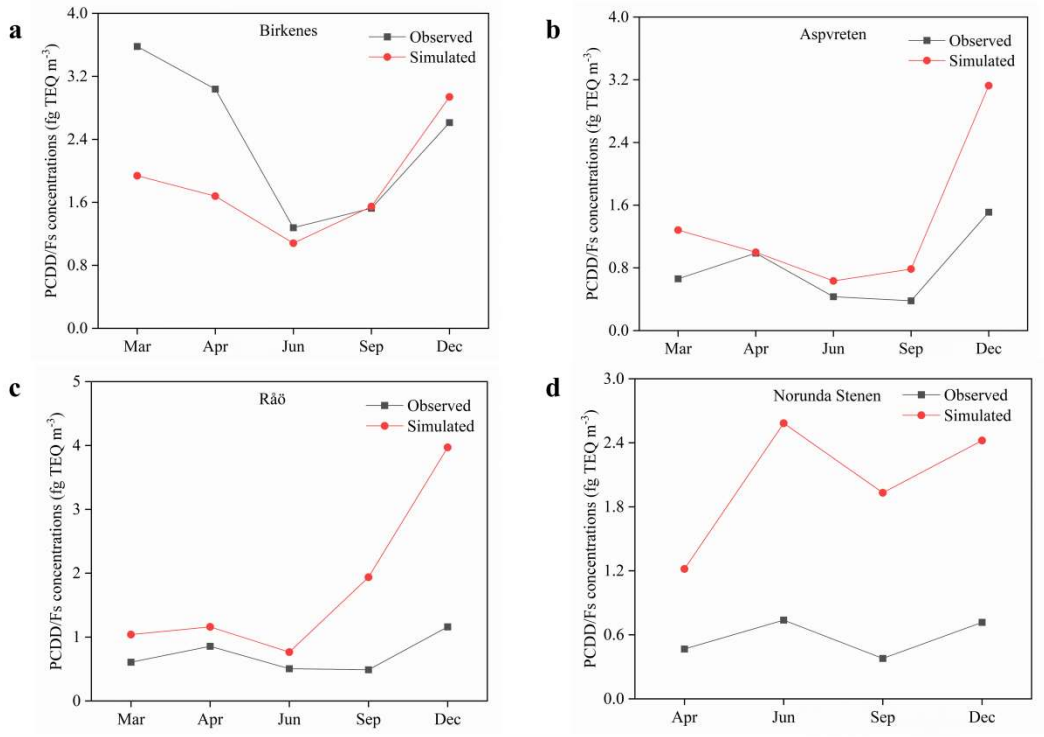

Figure S7. Comparisons between modeled and measured monthly mean air PCDD/Fs concentrations averaged for 2011–2012 at Birkenes (**a**), for 2016–2017 at Aspvreten (**b**), for 2016–2020 at Raö (**c**)and for 2018–2020 at Norunda Stenen (**d**), as marked with red triangle in **Figure S6a**.

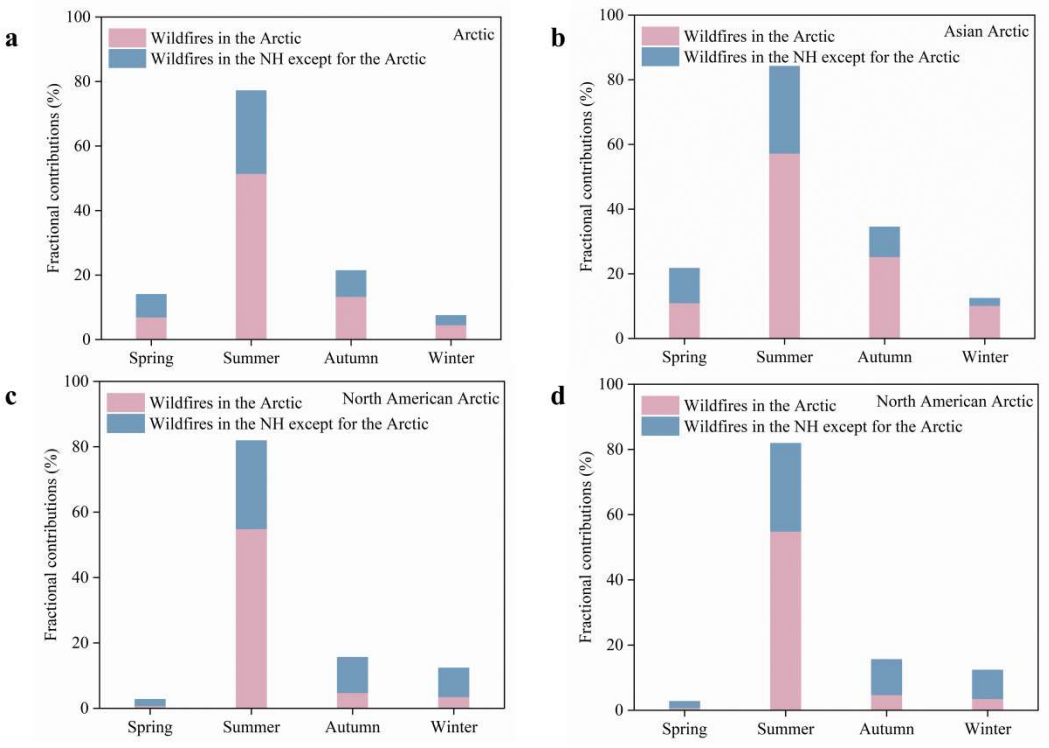

Figure S8. Seasonal variations in the contribution of the NH wildfire emissions to PCDD/Fs atmospheric concentrations averaged from 2011 to 2020 in the entire Arctic (**a**), the Asian Arctic (**b**), the North American Arctic (**c**), and the European Arctic (**d**).

References

[1] S. Song, K. Chen, T. Huang, J. Ma, J. Wang, X. Mao, H. Gao, Y. Zhao and Z. Zhou, *J. Hazard. Mater.*, 2023b, **443**, 130357.

[2] S. Song, B. Chen, T. Huang, S. Ma, L. Liu, J. Luo, H. Shen, J. Wang, L. Guo, M. Wu, X. Mao, Y. Zhao, H. Gao and J. Ma, *Environ. Sci. Ecotechnol.*, 2023, **14**, 100232.

[3] J. A. Prange, C. Gaus, R. Weber, O. Papke and J. F. Muller, *Environ. Sci. Technol.*, 2003, **37**, 4325–4329.

[4] C. Meyer, R. Black, K. Tolhurst, L. McCaw, G. Cook, R. Symons, et al., *Organohalogen Compd.*, 2007, **69**, 307–310.

[5] R. R. Black, C. P. Meyer, A. Touati, B. K. Gullett, H. Fiedler and J. F. Mueller, *Chemosphere*, 2011, **83**, 1331–1338.

[6] B. Gullett and A. Touati, *Atmos. Environ.*, 2003, **37**, 803–813.

[7] United Nations Environment Programme (UNEP), *Toolkit for Identification and Quantification of Releases of Dioxins, Furans and Other Unintentional POPs under Article 5 of the Stockholm Convention*, 2013.

[8] B. Gullett, A. Touati and L. Oudejans, *Atmos. Environ.*, 2008, **42**, 7997–8006.